Supporting Information

Title: Enhanced CO_2 Capture Capacities and Efficiencies with N-Doped Nanoporous Carbons Synthesized from Solvent-Modulated, Pyridinedicarboxylate-Containing Zn-MOFs

Authors: Jongsik Kim, Allen. G. Oliver, and Jason C. Hicks*

Contents

Experimental and Characterization

Chemicals

The following materials were purchased commercially and used as received: DMSO-*d6* (Alfa-Aesar, 99.5 atom %D), 2,5-pyridinedicarboxylic acid (Alfa Aesar, > 98.0 %), 1,4-benzenedicarboxylic acid (Aldrich, 99 %), 4,4'-bipyridine (Chem. Inpex International, 99 %), 2-methylimidazole (Alfa, Aesar, 97 %), pyridine (EMD, ACS grade), $Zn(NO_3)_2•6H_2O$ (Alfa Aesar, 99 %, metal basis), N,N-dimethylformamide (EMD, ACS grade), chloroform (Alfa-Aesar, ACS grade, > 99.8 %), methanol (BDH, ACS grade), hydrochloric acid (EMD, ACS grade, ~37 %), nitric acid (Sigma-Aldrich, ACS grade, ~70 %), and 4-aminobenzenesulfonamide (Sigma-Aldrich, 98 %).

Synthesis of Zn-MOFs

All Zn-MOFs were synthesized using a solvothermal method. For the synthesis of Zn-MOFs, optimized molar amounts of organic linker and $Zn(NO_3)_2•6H_2O$ were dissolved in specific amount of solvent (Table S2). This mixture was heated at predetermined temperature and time in a Schott Duran bottle under autogenous pressure (Table S2). After cooling to room temperature, the liquid was decanted, and the resulting crystals were filtered and washed with fresh DMF several times to form as-synthesized Zn-MOFs. The successful synthesis of BMOF-BDC and ZIF-8 was confirmed by their XRD patterns, which were in good agreement with those simulated (Fig. S8, CCDC No.: 255614 for BMOF-BDC; 602542 for ZIF-8).

Supercritical CO_2 extraction (Sc CO_2) process

As-synthesized ZnMOF-PDC materials were desolvated using a Sc CO_2 process based on a modified procedure previously reported by Kim and co-workers.[1] Prior to carrying out Sc CO_2 process, a guest solvent filling the pores of the as-synthesized ZnMOF-PDC material was exchanged using chloroform under ambient condition (once per day) for three days. In a typical Sc CO_2 process, 0.1 g of chloroform-exchanged ZnMOF-PDC material was loaded in a 20 mL vial and transferred into a stainless steel autoclave reactor (Parr 4590) manipulated by PID controller. The reactor was purged with 2 MPa of gaseous CO_2 three times before it was pressurized to 6.2 MPa of CO_2 at 25 °C without stirring. Then, the reactor was heated to 150 °C, resulting in a pressure of 7.5 MPa inside the reactor. This temperature and pressure indicated an atmospheric transformation of the reactor from a gaseous CO_2 to a supercritical CO_2. After holding the reactor under this condition for 30 minutes, the pressure was slowly released to 0 MPa (gauge pressure) before the temperature was cooled to 25 °C.

Preparation of carbons

As-synthesized Zn-MOFs were loaded into a tube furnace and subjected to the pyrolysis under the following condition: 30 mL min^{-1} of Ar flow, heated at a ramp rate of 10 °C min^{-1} to 1000 °C, and then held for 6 hours, which resulted in the formation of C_X materials, where X denotes the parent ZnMOF-PDC material prior to the pyrolysis (e.g., C_{Pyr-1} derived from as-synthesized Pyr-1). Carbon materials were also derived from other N-incorporating Zn-MOF materials (BMOF-BDC and ZIF-8) under the identical condition as that to prepare C_X materials. These were denoted as C_Y, where Y indicates the parent Zn-MOF material prior to the pyrolysis (e.g., C_{ZIF-8} derived from as-synthesized ZIF-8). It should be noted that, instead of using a low pyrolysis temperature (≤ 910 °C) that requires severe HCl etching to eliminate Zn by-products, we used 1000 °C as the pyrolysis temperature for the *in situ* elimination of Zn via evaporation, thereby minimizing the chance to neutralize Lewis basic N species with the partial collapse of porous carbon architecture.[2, 3]

Characterization

The surface areas and pore volumes of materials were estimated via the adsorption of N_2 at -196 ˚C using a Quantachrome NOVA 2200e. Materials were dried under 10^{-3} Torr dynamic vacuum at 125 °C overnight. Surface area of materials was estimated using nonlocal density functional theory (NLDFT), giving the value of S_{NLDFT}, while taking account of pressure range of $1\times10^{-7} < P/P_0 < 1.0$. Pore volume ($V_{PORE}$) of materials was also evaluated using NLDFT under the assumption that all pores were slit-shaped nanopores. X-ray diffraction (XRD) pattern was acquired using a D8 Advance Davinci diffractometer operated at 40 kV and 40 mA with monochromated CuKα radiation (λ = 1.5418 Å) at a scan speed of 0.75 second per step and a step size of 0.02° per step. ^{1}H-nuclear magnetic resonance spectroscopy (^{1}H-NMR) analysis was performed on a Bruker AVANCE III HD 400 using DMSO-*d6* as an analysis solvent. Scanning electron microscopy (SEM) analysis was performed on a Magellan 400. High resolution transmission electron spectroscopy (HRTEM) analysis was conducted on a FEI Titan Microscope with an operating voltage of 30 keV. The carbon material was suspended in an acetone and dispersed onto a copper grid supported on a holey carbon prior to the dryness under vacuum overnight for HRTEM analysis. X-ray photoelectron spectroscopy (XPS) analysis of carbons was performed using a PHI VersaProbe II X-ray photoelectron spectrometer. Each measurement was done under ultra-high vacuum (10^{-8} Torr) with a carbon dispersed on double sided carbon tape. The binding energy of the C 1s shell of amorphous carbon was employed as a reference located at binding energy of 284.5 eV. Thermogravimetric analysis (TGA) was performed using a Mettler-Toledo TGA/DSC STAR System under a N_2 atmosphere. Elemental analysis (EA) of carbons was carried out on a ECS 4010 (Costech Analytical Technologies, Inc) to obtain the bulk contents of C, H, and N. A tin capsule (3.3×5 mm, CE Elantech) was used to load the carbon (2-3 mg), where contents of C, H, and N were unknown. 4-aminobenzenesulfonamide (41.85 wt. % of C; 4.68 wt. % of H; 16.27 wt. % of N) was applied as an external standard to generate calibration curves for these components.

Structural refinement of BPyr-1 via single crystal XRD analysis

The structure of BPyr-1 was elucidated via single crystal X-ray diffraction (XRD) analysis. Refinement details and data for the structural determination of ZnMOF-PDC *iso*-structural to BPyr-1 can be found in our previous study.[4]

Quantification of the molar amount of DMF innate to ZnMOF-PDC materials

The molar amount of DMF (x) incorporated into the base unit ($Zn_2(PDC)_2(DMF)_x$) of ZnMOF-PDC materials was determined based on ^{1}H-NMR spectra of these materials digested using 1M HCl solution. For their digestion, 10 mg of ZnMOF-PDC material was dissolved in 0.5 g of HCl solution. After 10 minutes, in which ZnMOF-PDC material was completely decomposed to form clear solution, 0.5 g of DMSO-*d6* was added. The resulting solution was analyzed using ^{1}H-NMR spectroscopy. Based on one of protons present on PDC (organic linker of ZnMOF-PDC) after the digestion assigned as 'c' in Fig. S2, the molar amount of DMF (x) could be obtained by averaging two values calculated using the equation (1) and (2). This measurement of each material was conducted twice to get an average value of x.

$$mole\ of\ DMF\ using\ peak\ assigned\ as\ '3' = \frac{2H\ (moles\ of\ 'c')}{area\ of\ 'c'} \times \frac{area\ of\ '3'}{1H\ (mole\ of\ '3')}\ (1)$$

$$mole\ of\ DMF\ using\ peaks\ assigned\ as\ '1\&\ 2' = \frac{2H\ (moles\ of\ 'c')}{area\ of\ 'c'} \times \frac{area\ of\ '1\&\ 2'}{6H\ (moles\ of\ '1\&\ 2')}\ (2)$$

The molar amount of DMF incorporated into the base units of ZnMOF-PDC materials was also estimated using TGA analysis under an air atmosphere (10 mL min^{-1}). Based on the fact that ZnO was obtained as the final residual at high TGA temperatures (Fig. S4b), we calculated the amount of Zn (wt. %), which corresponded to the Zn contents included in the specific base unit ($Zn_2(PDC)_2(DMF)_x$) of ZnMOF-PDC materials (Table S3).

Low pressure CO_2 uptake measurements

CO_2 (99.99 %, Airgas) adsorption isotherms of carbons over the relative pressure (P/P_0) range between 1×10^{-3} to 1.0 were obtained on a Micromeritics ASAP 2020 instrument. The carbon was loaded into a bulb, capped with a TranSeal, and thoroughly degassed at 150 °C for 4 hours until the outgas rate was below 0.001 mmHg min^{-1}. After degassing the carbon, it was transferred into an analysis port, soaked in Dewar filled with D. I. water, iced D. I. water, or NaCl combined with iced D. I. water, and analyzed at 24 °C, 2 °C, or -10 °C, respectively. The retention of a bulb temperature was confirmed using a thermometer showing the deviation of temperature was ± 0.5 °C throughout the entire analysis.

Estimation of isosteric heat of CO_2 adsorption

Isosteric heats ($-Q_{ST}$) of CO_2 for carbons were evaluated using their adsorption isotherms measured at -10, 2, and 24 °C. The isotherms of these carbons were best-fitted using the Toth equation (3) composed of two parameters, such as c (bar^{-1}) and d describing the surface heterogeneity.[5, 6] In (3), N_a and N_{a0} denote the absolute and maximum amount of CO_2 adsorbed, whereas P indicates pressure (bar). Values of $-Q_{ST}$ for these materials were then determined using Clausius-Clapeyron equation (4),[4, 7] in which fitted parameters were applied to obtain values of ln (P) at the same value of N_a measured at three different temperatures in these materials (Fig. S12 and Table S4). In (4), P_1 indicates the pressure at T_1, whereas P_2 indicates the pressure at T_2. R denotes the ideal gas constant (8.3145 J $(K\bullet mol)^{-1}$). The Toth equation gave three values of $–Q_{ST}$ at specific value of N_a for each carbon due to the nature of c and d that are dependent on the measurement temperature.[5, 6] These three different values of $–Q_{ST}$ for each carbon were then averaged to depict the change of $–Q_{ST}$ with the value of N_a (Fig. S13).

$$N_a = N_{a0} \times \frac{c \times P}{(1 + (c \times P)^d)^{(\frac{1}{d})}} \ (3)$$

$$\ln\left(\frac{P_1}{P_2}\right) = \frac{Q_{st}}{R} \times \left(\frac{T_1 - T_2}{T_1 T_2}\right) (4)$$

Evaluation of Longevity for CO_2 uptake

Long-term recyclability of CO_2 uptake performance for carbons was estimated at 50 °C using a Mettler-Toledo TGA/DSC STAR System based on a modified procedure proposed by Tour and co-workers.[8] Prior to this measurement, a material was pretreated at 125 °C for 30 minutes under a N_2 atmosphere to remove H_2O and residual CO_2. After being cooled to 50 °C, 1 atm of CO_2 was dosed to the material for 10 minutes followed by heating the material at 100 °C for 10 minutes under the N_2 atmosphere. This CO_2 charge/discharge cycle was repeated thirty times. CO_2 uptake capacitance of the carbon at each cycle was calculated using the difference of weight before and after CO_2 uptake.

Table S1 H_2SO_4-based ILs to form carbons via pyrolysis at 1000 °C.[9]

	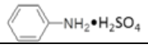	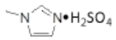	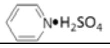
N source (mmol N g^{-1}) in IL	5.2	10.4	5.6
bulk N (mmol N g^{-1}) in carbon [a]	2.4	2.1	4.0
N_{eff}	46.5	20.6	72.1

[a] by EA.

Table S2 Synthetic parameters of Zn-MOFs.

Zn-MOF	$Zn(NO_3)_2•6H_2O$ (mmol)	organic linker (mmol) [a]	additive (mmol)	solvent (mL)	temperature (°C)	time (hours)
ZnMOF-PDC	4	PDC (2)	-	DMF (200)	100	18
Pyr-1	4	PDC (2)	pyridine (2)	DMF (200)	100	18
Pyr-2	4	PDC (2)	pyridine (4)	DMF (200)	100	18
Pyr-3	4	PDC (2)	pyridine (6)	DMF (200)	100	18
BPyr-1	4	PDC (2)	4,4′-bipyridine (2)	DMF (200)	100	18
BPyr-2	4	PDC (2)	4,4′-bipyridine (4)	DMF (200)	100	18
BPyr-3	4	PDC (2)	4,4′-bipyridine (6)	DMF (200)	100	18
BMOF-BDC	0.6	BDC (0.6) and 4,4′-bipyridine (0.3)	-	mixture of DMF and MeOH (12, v/v= 1:1)	120	48
ZIF-8 [b]	1.18	2-MIM (2.44)	-	DMF (15)	120	24

[a] abbreviation: PDC (2,5-pyridinedicarboxylate); BDC (1,4-benzenedicarboxylate); 2-MIM (2-methylimidazole). [b] three drops of 69 % HNO_3 were added right after dissolving $Zn(NO_3)_2•6H_2O$ and 2-MIM.

Table S3 The amount of DMF incorporated into Sc-CO_2 subjected ZnMOF-PDC ($Zn_2(PDC)_2(DMF)_x$) materials using ^{1}H-NMR and TGA analysis.

material	observed amount of DMF (x)	
	^{1}H-NMR [a]	TGA [b]
ZnMOF-PDC	1.14	1.12
Pyr-1	1.05	1.04
Pyr-2	1.00	0.99
Pyr-3	0.99	0.97
BPyr-1	0.94	0.93
BPyr-2	0.91	0.90
BPyr-3	0.92	0.90

[a] see Fig. S2. [b] see Fig. S4.

Table S4 Coefficients for Toth fitting of CO_2 adsorption isotherms of carbons.

carbon	temperature (°C)	coefficient [a]		
		N_{a0}	c	d
$C_{\text{ZnMOF-PDC}}$	-10	677.3740981	1.647146506	0.134824325
	2	1841.016	0.566665	0.118336
	24	14.81339	1.352215	0.318776
$C_{\text{Pyr-1}}$	-10	138.9921959	3.104817908	0.187317061
	2	383.8637	1.347	0.151708
	24	14.76527	3.565093	0.273437
$C_{\text{Pyr-2}}$	-10	119.6471939	3.014560531	0.197719422
	2	159.1449	1.970977	0.179626
	24	4.24498	2.489966	0.639785
$C_{\text{BPyr-1}}$	-10	77.61165418	4.823775889	0.202173878
	2	32.0891	2.109686	0.296972
	24	33.9535	2.909279	0.231777
$C_{\text{BPyr-2}}$	-10	125.1536501	3.104619625	0.187306322
	2	366.0691	1.335191	2.726007
	24	31.5695	2.726007	0.215802
$C_{\text{BMOF-BDC}}$	-10	27.07805686	3.952527904	0.315834868
	2	5.514724	3.097457	0.871907
	24	1.94017	3.090763	0.817433
$C_{\text{ZIF-8}}$	-10	158.602	5.496941	0.161839
	2	173.0342	2.787226	0.159263
	24	91.66236	4.044565	0.16483

[a] see equation (3).

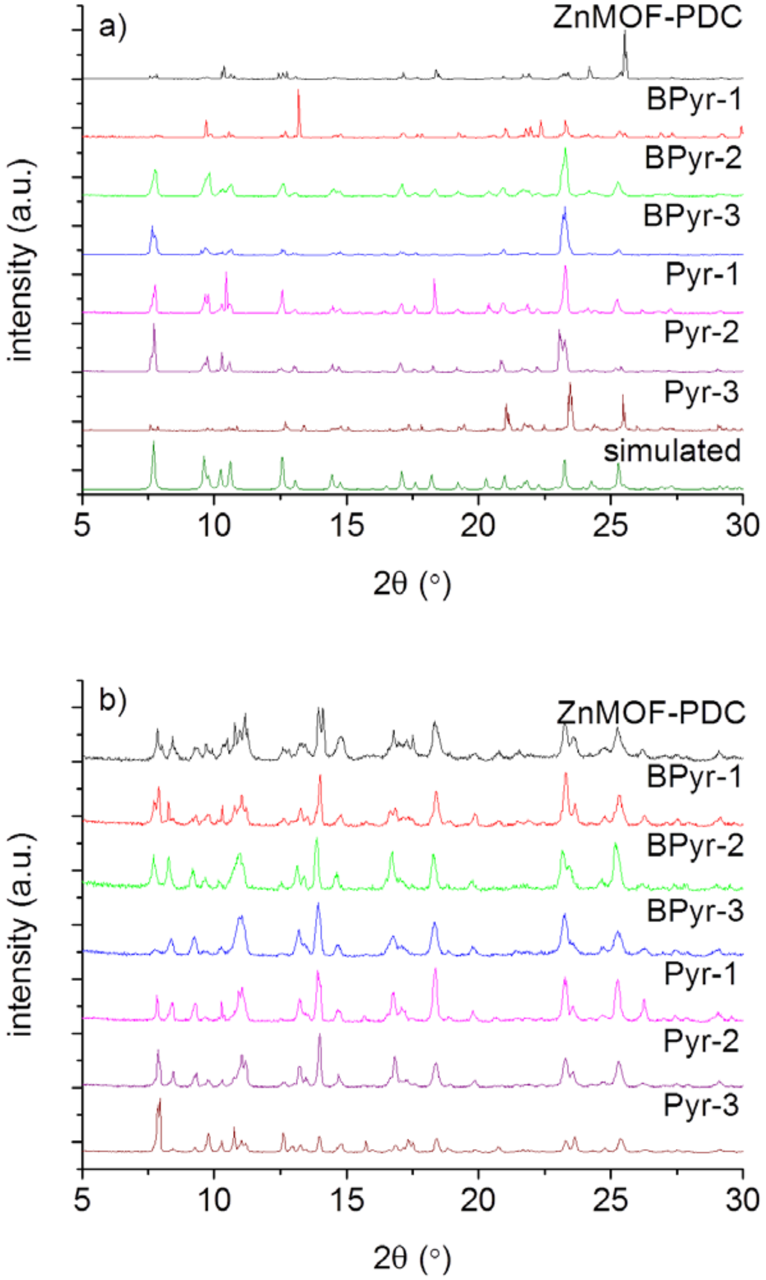

Fig. S1 XRD patterns of ZnMOF-PDC materials (a for as-synthesized; b for Sc CO_2-subjected).

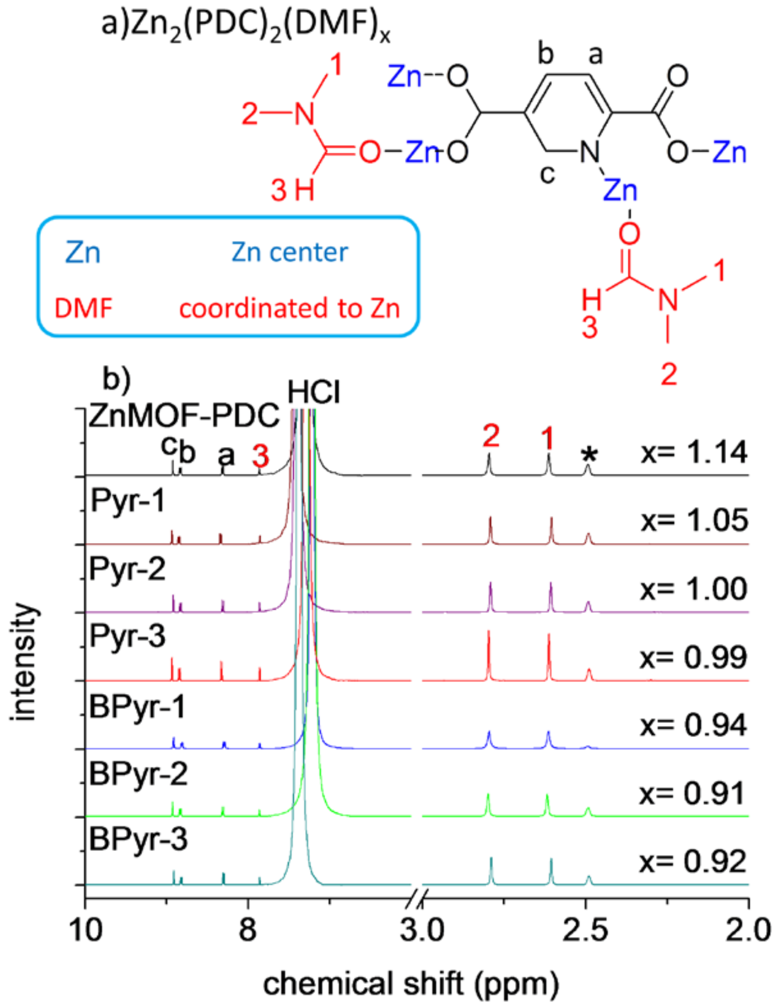

Fig. S2 a) Proposed base unit ($Zn_2(PDC)_2(DMF)_x$) of ZnMOF-PDC materials after being subjected to Sc CO_2 process. b) ^{1}H-NMR spectra of ZnMOF-PDC materials digested using 1M HCl solution (NMR solvent: DMFO-*d6*, shown as asterisk). x denotes the molar amount of DMF innate to ZnMOF-PDC materials.

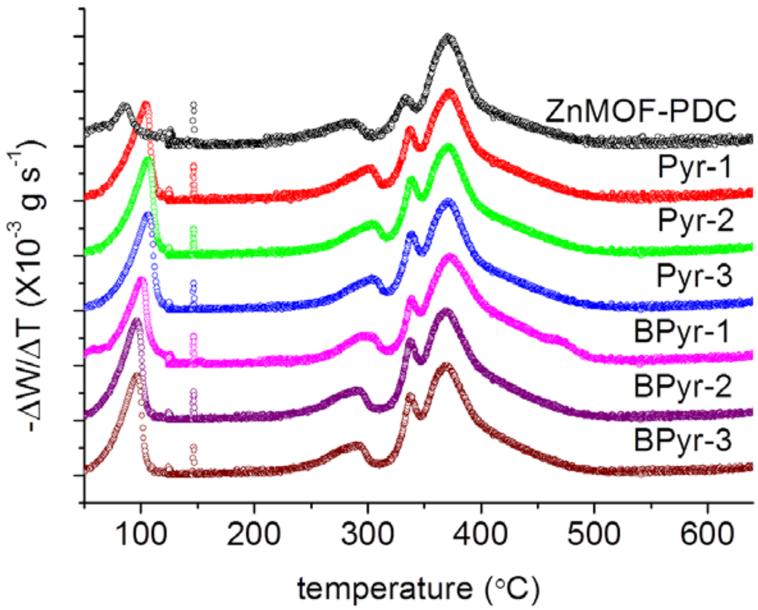

Fig. S3 DTG profiles of Sc CO_2-subjected ZnMOF-PDC materials under a N_2 atmosphere.

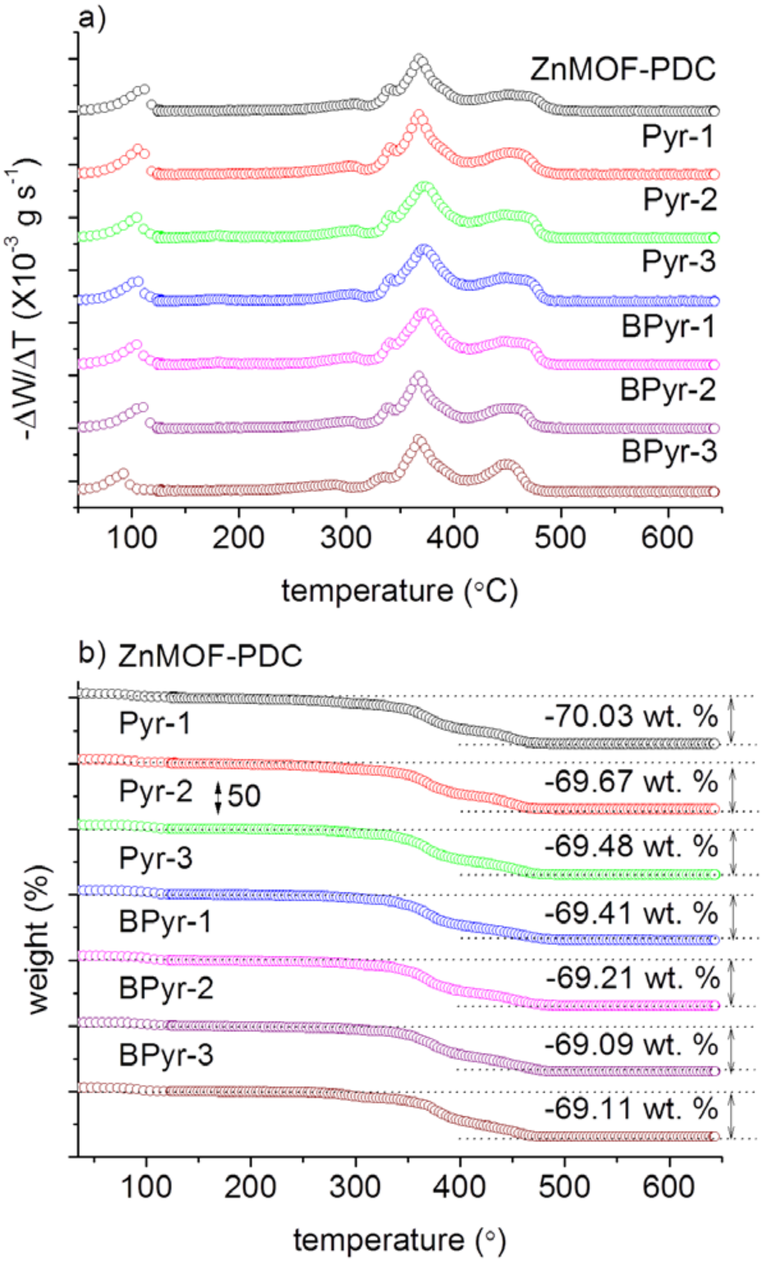

Fig. S4 a) DTG and b) TGA profiles of Sc CO_2-subjected ZnMOF-PDC materials under an air atmosphere.

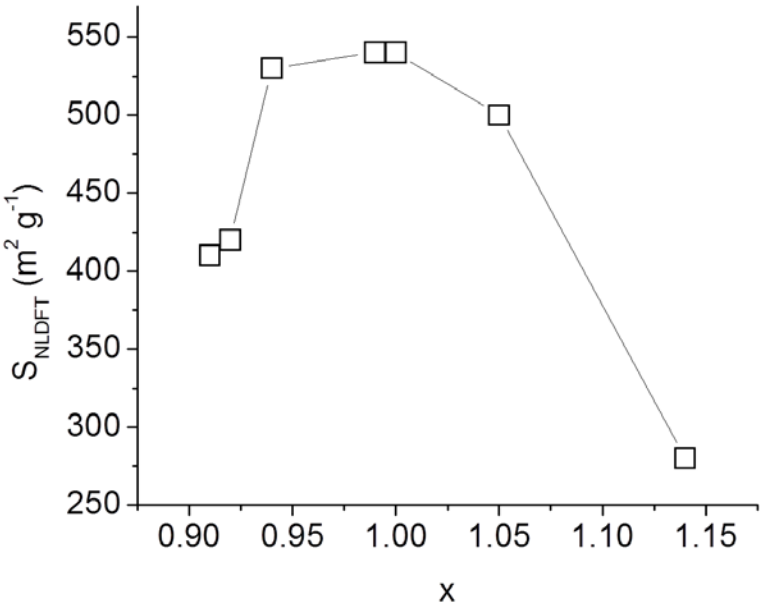

Fig. S5 S_{NLDFT} of ZnMOF-PDC ($Zn_2(PDC)_2(DMF)_x$) materials versus the molar amount of DMF (x) innate to these materials.

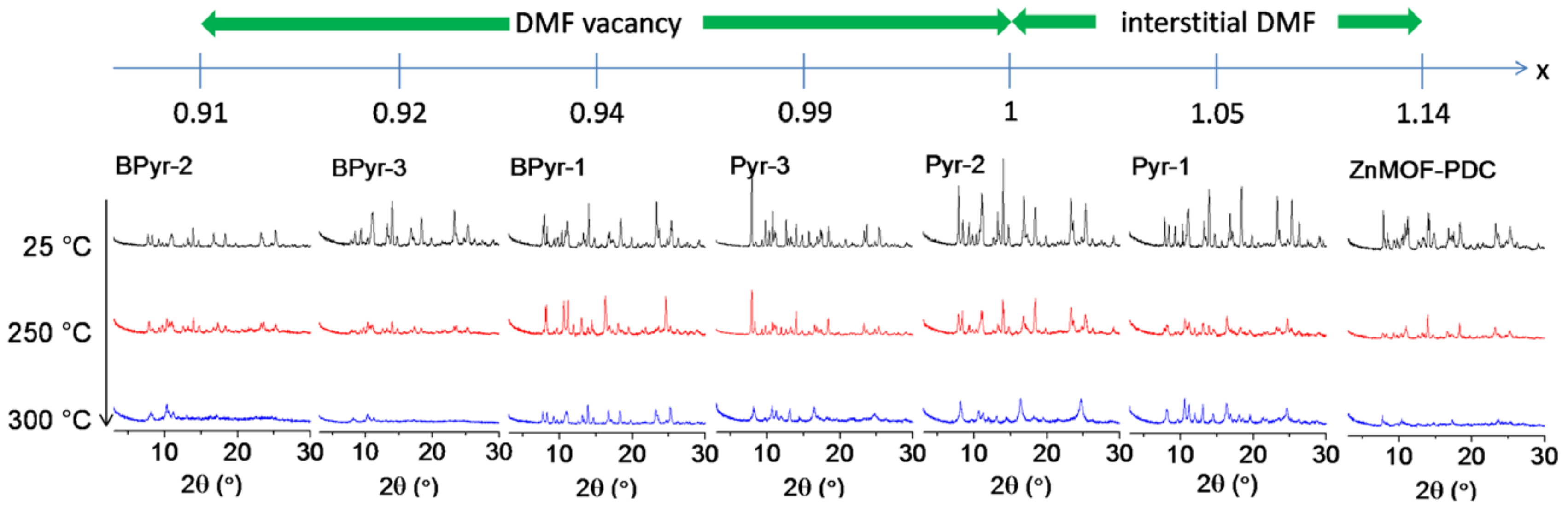

Fig. S6 Normalized XRD patterns of ZnMOF-PDC ($Zn_2(PDC)_2(DMF)_x$) materials after thermolysis at 250 and 300 °C under an Ar atmosphere. These patterns were obtained using an identical amount (~30 mg) of ZnMOF-PDC materials. These were normalized based on the XRD pattern of Pyr-2 at 25 °C showing the highest intensity among ZnMOF-PDC materials synthesized in this study.

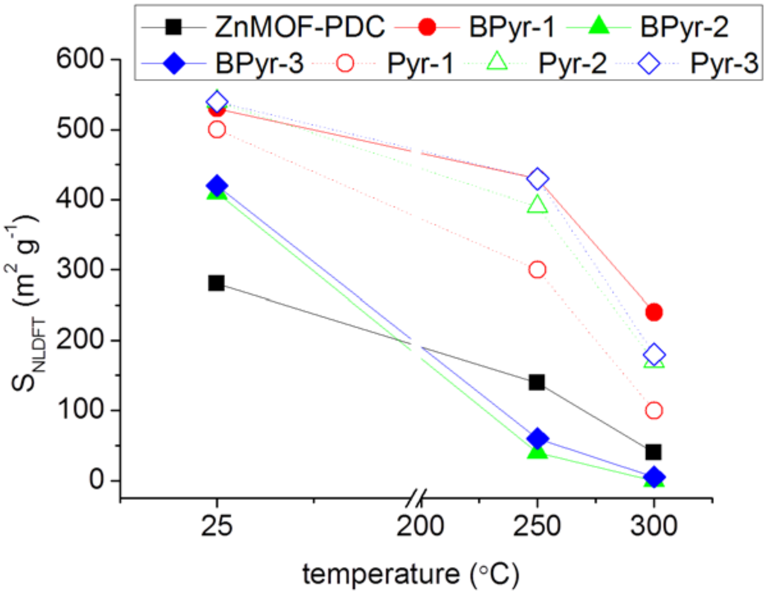

Fig. S7 S_{NLDFT} of ZnMOF-PDC materials versus thermolysis temperature.

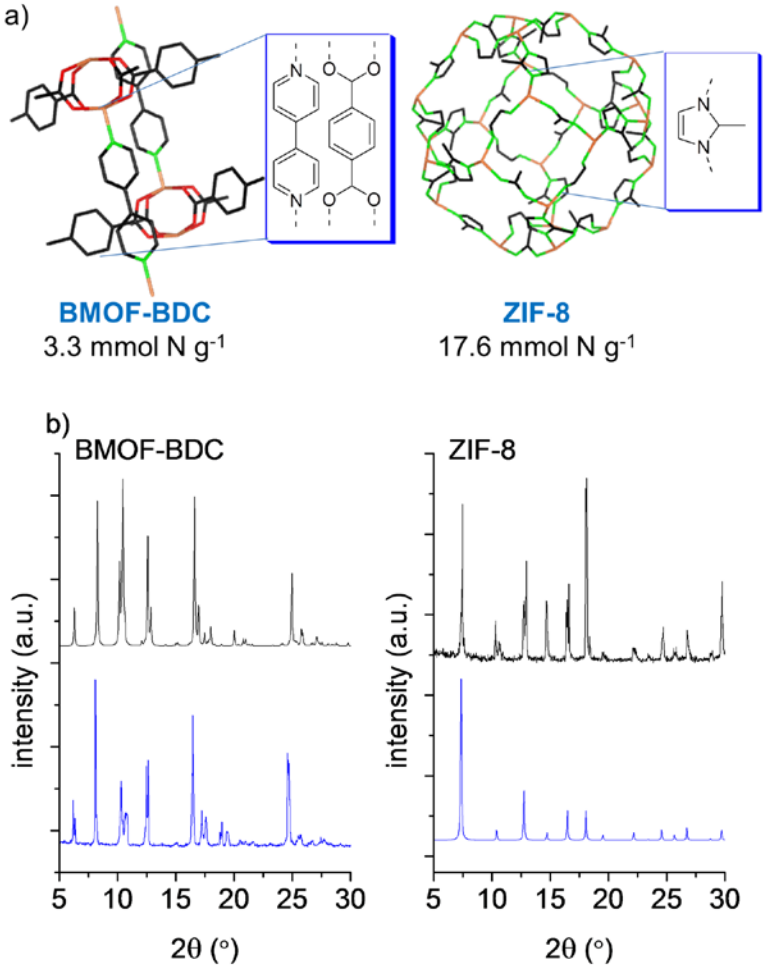

Fig. S8 a) Base units of BMOF-BDC and ZIF-8. b) XRD patterns of as-synthesized BMOF-BDC and ZIF-8 (black) and their simulated patterns (blue).

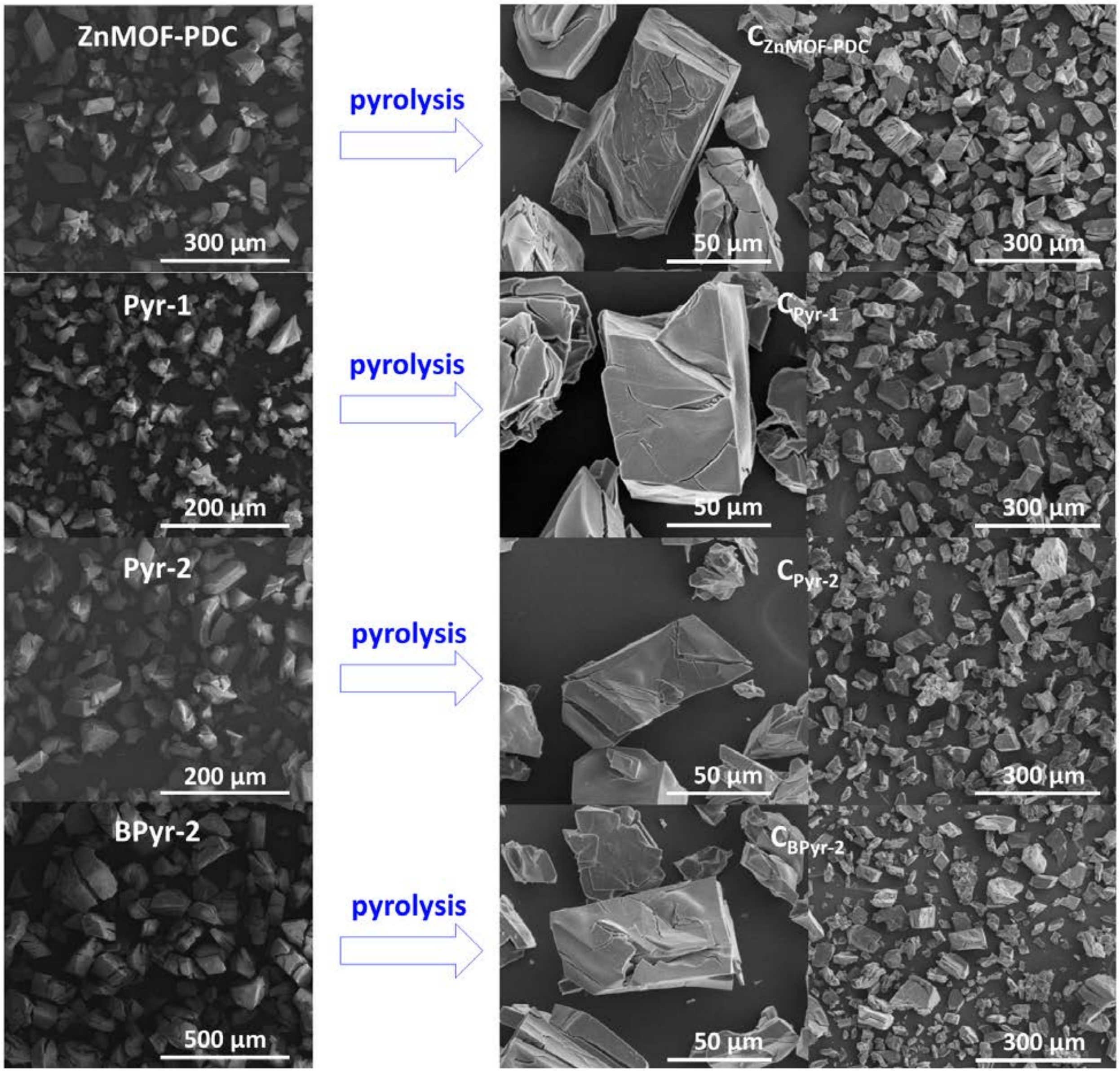

Fig. S9 SEM images of ZnMOF-PDC materials and corresponding carbons.

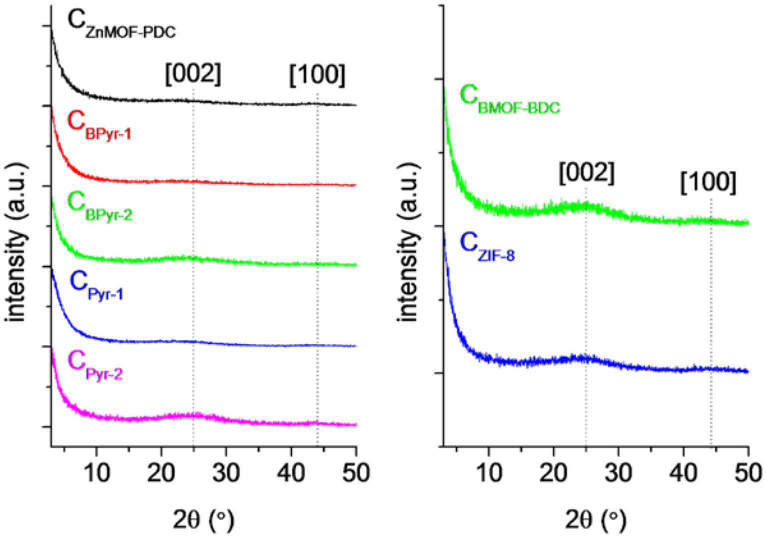

Fig. S10 XRD patterns of carbons.

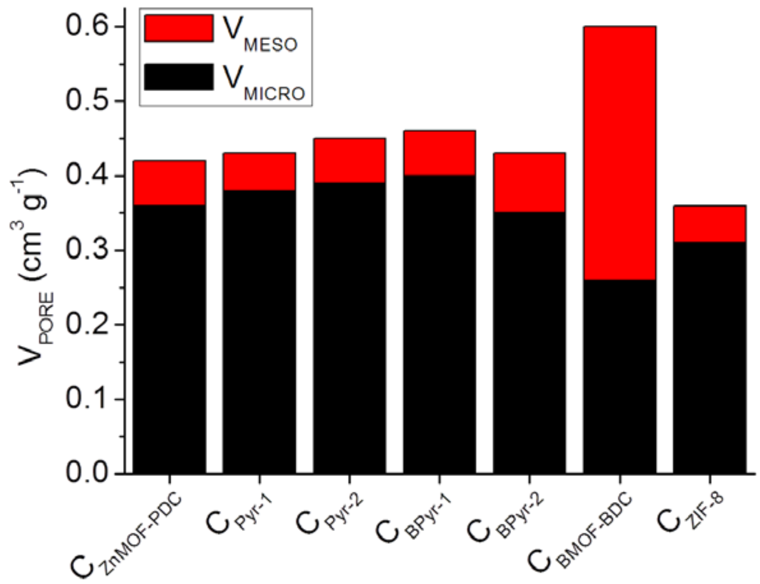

Fig. S11 Pore characteristics of carbons.

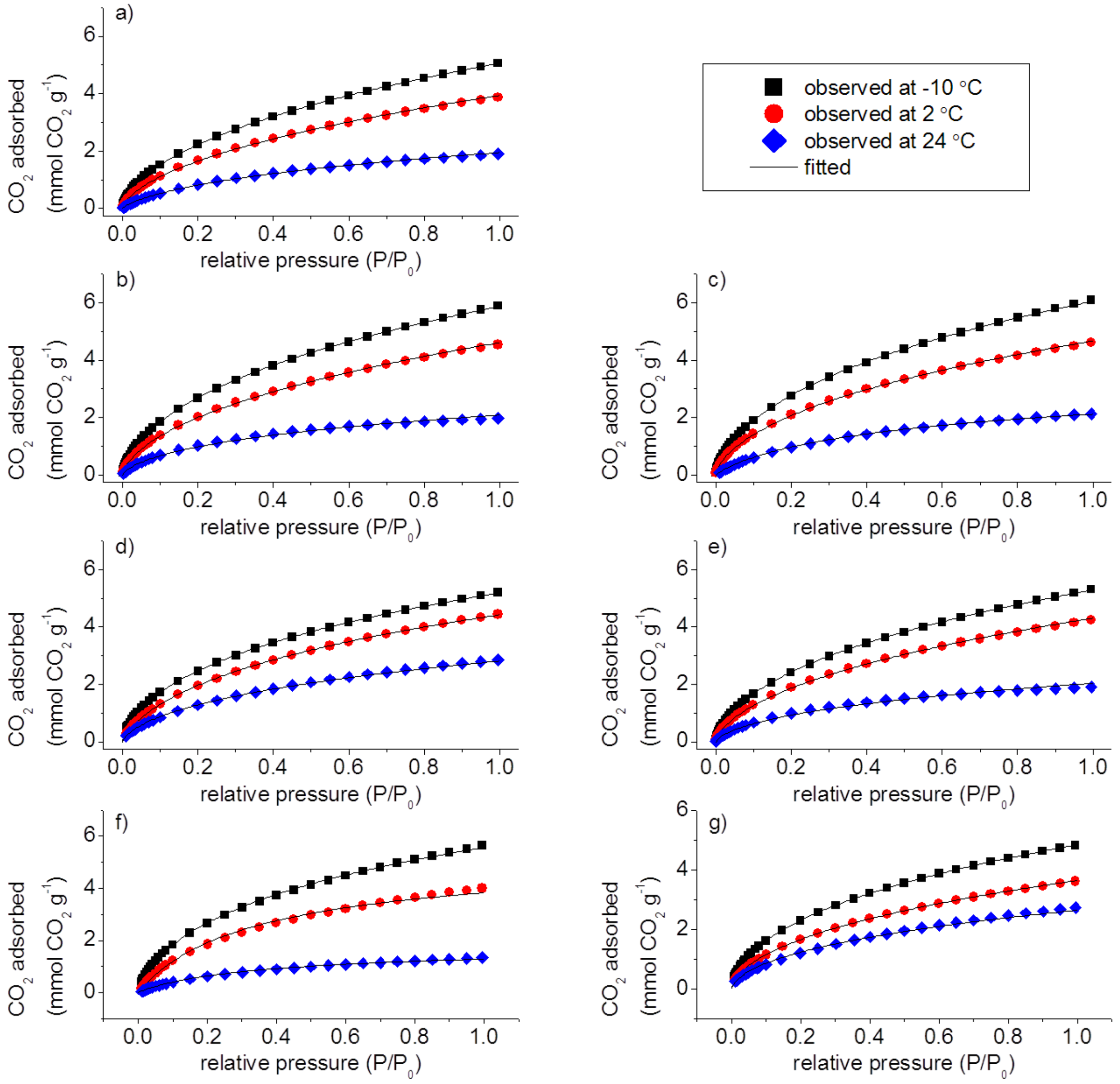

Fig. S12 Low pressure CO_2 adsorption isotherms of carbons with Toth fitting: a) $C_{ZnMOF-PDC}$, b) C_{Pyr-1}, c) C_{Pyr-2}, d) C_{BPyr-1}, e) C_{BPyr-2}, f) $C_{BMOF-BDC}$, and g) C_{ZIF-8}.

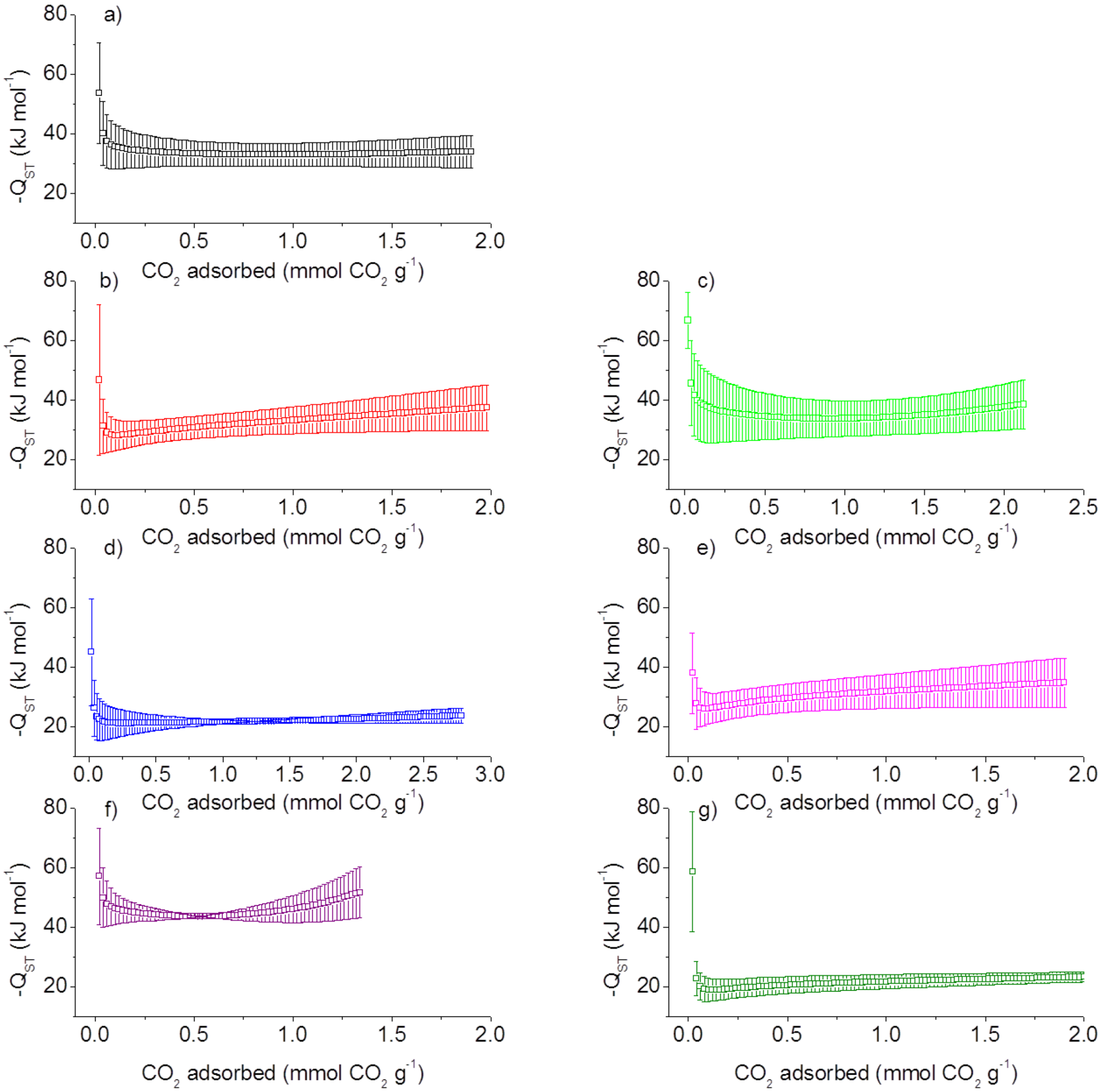

Fig. S13 Isosteric heat of CO_2 adsorption (-Q_{ST}) for carbons: a) $C_{ZnMOF\text{-}PDC}$, b) $C_{Pyr\text{-}1}$, c) $C_{Pyr\text{-}2}$, d) $C_{BPyr\text{-}1}$, e) $C_{BPyr\text{-}2}$, f) $C_{BMOF\text{-}BDC}$, and g) $C_{ZIF\text{-}8}$.

References

1. J. Kim, D. O. Kim, D. W. Kim and K. Sagong, *J. Solid State Chem.*, 2013, 197, 261-265.
2. R. Verdejo, S. Lamoriniere, B. Cottam, A. Bismarck and M. Shaffer, *Chem. Commun.*, 2007, DOI: 10.1039/b611930a, 513-515.
3. Z. Wang, M. D. Shirley, S. T. Meikle, R. L. D. Whitby and S. V. Mikhalovsky, *Carbon*, 2009, 47, 73-79.
4. J. Kim, A. G. Oliver, G. T. Neumann and J. C. Hicks, *Eur. J. Inorg. Chem.*, 2015, DOI: 10.1002/ejic.201500245.
5. G.-P. Hao, W.-C. Li, D. Qian, G.-H. Wang, W.-P. Zhang, T. Zhang, A.-Q. Wang, F. Schüth, H.-J. Bongard and A.-H. Lu, *J. Am. Chem. Soc.*, 2011, 133, 11378-11388.
6. R. Hoseinzadeh Hesas, A. Arami-Niya, W. M. A. Wan Daud and J. N. Sahu, *J. Ind. Eng. Chem.*, DOI: http://dx.doi.org/10.1016/j.jiec.2014.09.029.
7. H. J. Park and M. P. Suh, *Chem. Sci.*, 2013, 4, 685-690.
8. C.-C. Hwang, Z. Jin, W. Lu, Z. Sun, L. B. Alemany, J. R. Lomeda and J. M. Tour, *ACS Appl. Mater. Interfaces*, 2011, 3, 4782-4786.
9. S. Zhang, K. Dokko and M. Watanabe, *Chem. Mater.*, 2014, 26, 2915-2926.